Biochimica et Biophysica Acta, 1028 (1990) 103–109
Elsevier

BBAMEM 74997

Temperature dependence of the ripple structure in dimyristoylphosphatidylcholine studied by synchrotron X-ray small-angle diffraction

Sinzi Matuoka [1], Satoru Kato [1], Morio Akiyama [2], Yoshiyuki Amemiya [3], Ichiro Hatta [1]

[1] *Department of Applied Physics, Faculty of Engineering, Nagoya University, Nagoya,* [2] *Department of Physics, Sapporo Medical College, Sapporo and* [3] *Photon Factory, National Laboratory for High Energy Physics, Tsukuba, Ibaraki (Japan)*

(Received 17 January 1990)

Key words: Dimyristoylphosphatidylcholine; Ripple structure; Small angle X-ray diffraction

The ripple structure of 1,2-dimyristoyl-L-phosphatidylcholine (DMPC) multibilayer containing excess water (60 wt%) was studied by synchrotron X-ray small-angle diffraction. The (0,1) spacing which corresponds to the ripple repeat distance depends on temperature: At 13°C the (0,1) spacing is 14.15 nm, the spacing decreases at higher temperatures and reaches 12.1 nm at 23.5°C, just below the main transition temperature. The spacing is in good agreement between heating process and cooling process except for the supercooling region. The result suggests that the rearrangement of the ripple structure takes place during temperature change successively. The Landau-de Gennes free energy equation explains well the temperature dependence of the ripple repeat distance.

Introduction

Hydrated phosphatidylcholine (PC) multibilayer systems undergo well characterized phase transitions with the sequence of L_c, $L_{\beta'}$, $P_{\beta'}$ and L_α phases. In the $P_{\beta'}$ phase periodically undulated 'ripple' structure in the bilayer with a period of 12 nm–14 nm has been observed [1–6]. In the other phases the lipid bilayers possess a flat surface structure.

The ripple repeat distance has been obtained from X-ray diffraction and freeze-fracture electron microscopy experiments. Tardieu et al. have proposed a two-dimensional electron density profile of ripple structure from crystallographic data in dilauroylphosphatidylcholine (DLPC) and dimyristoylphosphatidylcholine (DMPC) [1]. Janiak et al. found by X-ray diffraction that the ripple repeat distance is 12 nm at 20°C in fully hydrated DMPC and have pointed out that it depends on the water content [2]. Using freeze-fracture electron microscopy, the ripple repeat distance in the fully hydrated DMPC system was reported to be 13 ± 2 nm, 12–14 nm, 13 ± 1 nm and 12.9 ± 1.7 nm by Sackmann et al. [6], Copeland and McConnell [7], Luna and McConnell [4] and Hicks et al. [3], respectively.

From the observation with the scanning tunneling microscope, Zasadzinski et al. have obtained that the ripple repeat distance of DMPC is 13 nm and the average amplitude is 4.5 nm [8].

Inoko et al. have described from their X-ray diffraction measurements that the ripple periodicity in the fully hydrated DPPC is insensitive to temperature [9]. On the basis of this fact Wack and Webb have focused on the concentration- and chain-length dependence in their recent report [10]. Mortensen et al. have studied the temperature dependence of dimyristoylphosphatidylcholine with perdeuterated fatty acid chains (DMPC-d_{54}) by small-angle neutron scattering [11]. Their experiments have been carried out for a 'stable' sample prepared by storing at 5°C for months and a 'metastable' sample which has not experienced the low temperature. The former undergoes subtransition and the latter does not. In our present study, the experiment was performed for the metastable sample in that sense. As far as judged from Fig. 10 of Ref. 11, there is scarcely temperature dependence of the ripple periodicity in the 'metastable' DMPC-d_{54}. However, we can read from Figs. 5 (b) and (c) of Ref. 11 that the ripple repeat distance becomes longer at lower temperatures. In order to make clear the uncertain situation, in this study we focused on the temperature dependence of

Abbreviations: DLPC, 1,2-dilauroyl-L-phosphatidylcholine; DMPC, 1,2-dimyristoyl-L-phosphatidylcholine; DPPC, 1,2-dipalmitoyl-L-phosphatidylcholine; PC, phosphatidylcholine; DSC, differential scanning calorimetry.

Correspondence: I. Hatta, Department of Applied Physics, School of Engineering, Nagoya University, Nagoya 464-01, Japan.

ripple periodicity, using synchrotron X-ray small-angle diffraction.

Marder et al. have discussed the ripple formation in terms of the phenomenological Landau-de Gennes theory, in which the order parameter is defined by the normalized bilayer thickness [12]. They have pointed out that the spatial modulation of the order parameter is essential to the formation of the ripple structure. Such spatial modulation is due to the fact that the ripple structure consists of periodically banded microdomain structures composed of fluid-like and gel-like regions. The coexistence of fluid-like and solid-like microdomains in the $P_{\beta'}$ phase has been suggested by nuclear magnetic resonance [13], fluorescence experiments [14] and electron spin resonance [15]. The temperature dependence of the ripple periodicity can be explained by the phenomenological Landau-de Gennes theory.

Materials and Methods

DMPC was purchased from Sigma Chemical Co. and also from Avanti Polar Lipids Co. Data shown in this manuscript were taken using the former sample, however, similar results were obtained for the latter one. The materials were found to be pure by thin-layer chromatography and then were used without further purification. For preparation of multilamellar liposomes, DMPC powder was first dissolved in spectroscopic-grade chloroform. After the chloroform was evaporated under a stream of nitrogen gas, the sample was dried under vacuum overnight to remove the trace of the solvent. They were hydrated with distilled water and incubated at about 50°C for 3–8 h. To obtain enough intensity in the X-ray diffraction measurement the sample was concentrated by centrifugation with $9000 \times g$ for 30 min. The water content in the sample was estimated by measuring the lipid weight before hydration and the total weight after centrifugation. The amount of lipid that remained in the supernatant was very small and thus was neglected. The water content thus estimated was 60 ± 1 wt%.

Synchrotron X-ray small-angle diffraction measurements were made at BL-15A Station at Photon Factory, National Laboratory for High Energy Physics in Tsukuba. Horizontally focused and monochromatized 0.155 nm X-ray beam was used for experiments. The design of the small-angle X-ray diffractometer has been described in Ref. 16 in detail. Diffraction patterns were detected with a one-dimensional position-sensitive proportional counter (Rigaku). Its effective length was 170 mm and the data profiles were recorded with 512 channels. The sample-to-detector distance was 1300 mm and then the maximum diffraction angle is $2\theta = 3.8°$. The lamellar first- and second-order diffraction could be measured with an angular resolution of 0.016°.

The sample cell consists of an aluminum plate of 1 mm thickness having a hole of 4×6 mm. The sample was set in the hole and sealed by Mylar films of 12 μm thickness in the both surfaces of the plate. This was fixed in a brass holder and immersed into the temperature-controlled water supplied from a temperature constant bath (NESLAB Co. Ltd., RTE-5B). The temperature of the sample was monitored with a chromel-alumel thermocouple situated near the plate.

X-ray diffraction profiles were taken with sampling time of 60 s. The temperature of the sample was changed step by step. At each step the temperature was kept constant within the stability of 0.1 C° and under this condition the X-ray diffraction measurement was carried out. The average heating rate resulted in 0.23 C°/min. After measurements in heating scan, the sample was incubated for an hour at 27.0°C which was 3 C° higher than main transition temperature. Before cooling the stage on which the sample cell holder was situated was translocated horizontally to avoid radiation damage. As in the case of the heating scan, the sample was cooled step by step and the average cooling rate was −0.23 C°/min.

Results

Fig. 1 shows the X-ray diffraction patterns of DMPC multibilayer containing 60 wt% water measured in the $P_{\beta'}$ phase. The profiles taken in cooling process from L_α to $P_{\beta'}$ are drawn. A small but distinct peak observed around $s(=2\sin\theta/\lambda) = 0.8 \cdot 10^{-1}$ (nm^{-1}) was assigned as the (0,1) peak corresponding to the ripple repeat distance. As far as the (0,1) peak is concerned, it reaches to the stable state at least within 1 min after the

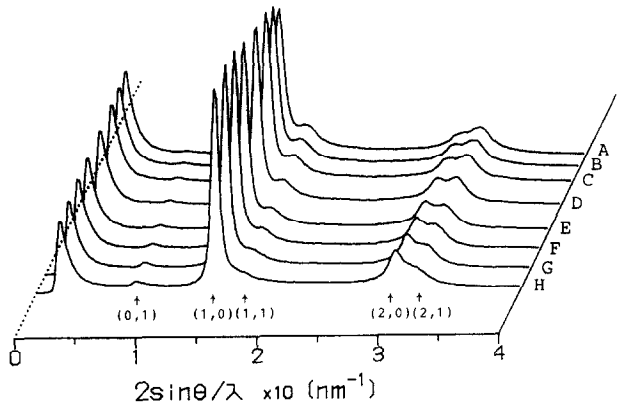

Fig. 1. The X-ray diffraction profiles of DMPC multibilayer containing 60 wt% water in the $P_{\beta'}$ phase. Measurements were made in the cooling process. The temperature change was performed step by step. The average temperature scanning rate was 0.23 C°/min. The sampling time of these profiles was 60 s. The observed five peaks are assigned as (0,1), (1,0), (1,1), (2,0) and (2,1) (see text). The intensity in the range from $s = 0$ to $0.2 \cdot 10^{-1}$ (nm^{-1}) is reduced due to a beam stopper. A, 13.0°C; B, 14.0°C; C, 15.2°C; D, 17.0°C; E, 19.0°C; F, 20.5°C; G, 22.0°C; H, 23.5°C.

temperature is changed in the $P_{\beta'}$ phase (data not shown). Furthermore, there is an intense peak assigned as the (1,0) peak corresponding to the lamellar repeat distance near $s = 1.5 \cdot 10^{-1}$ (nm^{-1}). At 23.5°C the (0,1) spacing is 12.1 nm and the (1,0) spacing is 6.74 nm which are in good agreement with that reported previously by Janiak et al. [2]. The peak appearing near $s = 3 \cdot 10^{-1}$ (nm^{-1}) is assigned as the (2,0) reflection. In addition to the above three peaks, another peaks are observed near $s = 1.71 \cdot 10^{-1}$ (nm^{-1}) and near $s = 3.1 \cdot 10^{-1}$ (nm^{-1}) as the shoulder of the (1,0) peak and (2,0) peak, respectively. The former one is indexed as the (1,1) peak according to the assignment in DMPC multibilayer containing 22.3 wt% water by Janiak et al. [5]. The latter peak is assigned as the (2,1) peak between two possibilities of (2,1) peak and (2, − 1) peak. Because the variance $\Sigma(d_{obs} - d_{cal})^2$ for the above-mentioned five peaks becomes smaller in the case that the peak is not assigned as the (2, − 1) but as the (2,1) peak. Here d_{cal} denotes the calculated spacings from lattice parameters a, b and γ of the monoclinic unit cell, where γ is the angle between the *a*-axis and the *b*-axis. d_{obs} is the observed spacing determined as follows. The diffraction peaks were assumed to be composed by superposition of Lorenzian profiles and analyzed by the least-squares fitting program developed by Nakagawa and Oyanagi [17].

In Fig. 2 the very small-angle region of the X-ray diffraction patterns of DMPC in cooling and heating runs are drawn using an expanded scale. It can be seen that with decreasing temperature the maximum of the peak shifts towards the small-angle direction both in heating and cooling. Owing to the detection of the profiles by PSPC, we could obtain the data points at every channel separately. Then we only distinguish the difference of the intensities between the neighboring channels whose distance was 0.37 nm at 13°C and 0.26 nm at 23.5°C. For the detailed analysis of the profile, a further study is necessary. In spite of the limitation as described above, plotting of the (0,1) spacings as a function of temperature (Fig. 3) clearly demonstrates that the temperature dependence obtained in heating process is basically similar to that obtained in cooling process. In the cooling run, however, the $P_{\beta'}$ phase has a supercooling region below 15°C.

The observed spacings of five peaks and the lattice parameters *a*, *b* and γ at various temperatures in the cooling process are summarized in Table I. The (1, − 1) and (2, − 1) spacings calculated from the lattice parameters are also given in this Table, however, these peaks are not observed due to the strong (1,1) and (2,1) peaks, respectively, lying near to the above peaks. The difference between the (0,1) spacing and the real ripple repeat distance (lattice parameter *a*) is estimated to be less than 0.1 nm. This is due to the fact that the angle γ is near 90°. From Fig. 3 it is concluded that the ripple

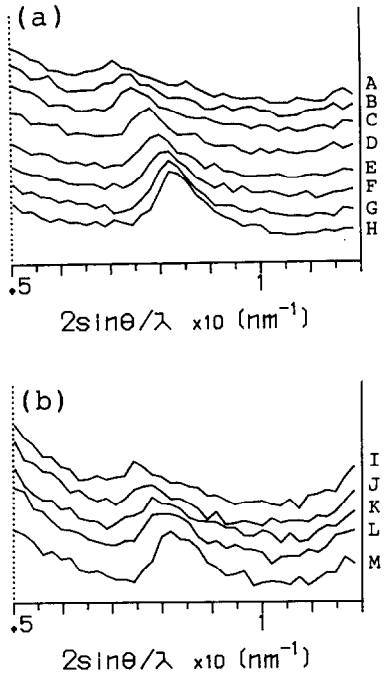

Fig. 2. The X-ray diffraction profiles of DMPC multibilayer in the small-angle region in cooling (a) and in heating (b). The (0,1) peak which corresponds to the ripple repeat distance can be seen in the region from $s = 0.7 \cdot 10^{-1}$ (nm^{-1}) to $0.9 \cdot 10^{-1}$ (nm^{-1}). A, B, C, D, E, F, G and H in (a) denote the results obtained at the same temperatures as indicated in Fig.1. In (b): I, 15.8°C; J, 16.8°C; K, 18.8°C; L, 20.3°C; M, 22.6°C.

repeat distance becomes longer from 12 nm to 14 nm as the temperature decreases. The other spacings do not show a significant temperature dependence.

On cooling the (0,1) peak was observed below to 13.0°C and therefore, the pretransition temperature lies below this temperature. It is rather difficult to infer the pretransition temperature from X-ray diffraction measurements, since the (0,1) peak intensity becomes weak and undetectable near the pretransition temperature.

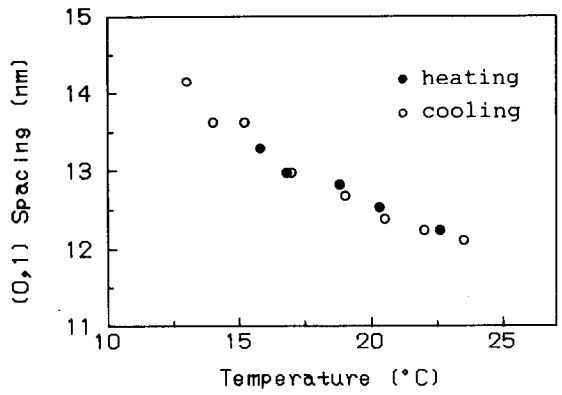

Fig. 3. Temperature dependence of the (0,1) spacing of the DMPC multibilayer measured by the small-angle X-ray diffraction. Open circles represent the data obtained in the cooling run with −0.23 C°/min. Closed circles represent the data obtained in the heating run with 0.23 C°/min.

TABLE I

The spacings of observed X-ray diffraction peaks and those calculated from lattice parameters a, b and γ of monoclinic unit cell

The (1, −1) and (2, −1) are not detectable, since they are hidden by the strong peaks of (1,1) and (2,1), respectively. Then they are denoted as a missing mark '–'.

	a (nm)	*b* (nm)	γ (°)	(0,1) (nm)	(1,0) (nm)	(1,1) (nm)	(1, −1) (nm)	(2,0) (nm)	(2, −1) (nm)	(2,1) (nm)
23.5°C obs.				12.11	6.74	5.86	–	3.37	–	3.19
cal.	6.74	12.11	90.7	12.11	6.74	5.86	5.92	3.37	3.26	3.24
22.0°C obs.				12.24	6.70	5.83	–	3.34	–	3.17
cal.	6.70	12.24	91.2	12.24	6.70	5.82	5.93	3.35	3.25	3.21
20.5°C obs.				12.38	6.69	5.83	–	3.34	–	3.17
cal.	6.70	12.38	91.4	12.38	6.69	5.83	5.95	3.35	3.25	3.21
19.0°C obs.				12.67	6.70	5.82	–	3.34	–	3.17
cal.	6.70	12.68	92.5	12.67	6.70	5.82	6.03	3.35	3.27	3.20
17.0°C obs.				12.97	6.72	5.84	–	3.35	–	3.17
cal.	6.73	12.98	93.1	12.96	6.72	5.83	6.10	3.36	3.29	3.21
15.2°C obs.				13.62	6.74	5.86	–	3.36	–	3.18
cal.	6.76	13.66	94.6	13.62	6.74	5.86	6.24	3.37	3.33	3.21
14.0°C obs.				13.62	6.76	5.86	–	3.36	–	3.18
cal.	6.78	13.67	94.8	13.62	6.76	5.86	6.27	3.38	3.35	3.22
13.0°C obs.				14.15	6.78	5.89	–	3.36	–	3.19
cal.	6.82	14.22	95.7	14.15	6.78	5.89	6.37	3.39	3.37	3.23

The pretransition temperature has been reported to be 10.9°C by DSC measurements [18] on cooling with a temperature scanning rate 0.25 C°/min. This is consistent with the present experiment. On heating the (1,0) peaks of the $L_{\beta'}$ and $P_{\beta'}$ phases coexist between 12.5°C and 15.0°C indicating that the pretransition occurs in this temperature range. From DSC measurements the pretransition takes place at 13.9°C on heating [18], which is also consistent with that obtained from the X-ray diffraction measurements.

Discussion

Synchrotron X-ray is very useful in the small-angle diffraction study, because the X-ray beam is coherent and its divergence is suppressed to low level. These properties make it possible to study the detailed behavior of the ripple peak because the background intensity is extremely small in comparison with the former experiments.

From the paper by Mortensen et al. [11] we have deduced, although they did not pay attention to this fact, that the ripple repeat distance in the metastable system of DMPC increases at lower temperature and the ripple peak intensity increases at higher temperature. These results are qualitatively in good agreement with ours. However, the ripple repeat distance calculated from Fig. 5 in Ref. 11 is rather large compared to that obtained by us. This may be due to the small fraction of water content; 17 wt% as reported by Janiak et al. [5].

Caffrey et al. [19] pointed out the effect of radiation damage caused by high intense X-ray such as synchrotron radiation and reported that a cumulative radiation dose larger than 10 Mrad yielded reduction of the peak intensity of lamellar reflection and increase of lamellar periodicity and turned finally into three diffuse peaks [12]. Regardless of such drastic structural changes the extent of DPPC breakdown was estimated to be only 10% [12]. In our experiments the maximum cumulative radiation dose was estimated to be less than 0.7 Mrad. We checked that such radiation dose produced no serious radiation damage in the DMPC system at 27°C (L_α phase), that is, the peak intensity did not become small, the lamellar spacing did not increase, and the diffuse peaks did not appear. Taking into account our radiation dose in this experiment, the impurity produced by the X-ray may be less than 1%. From the reversibility of the ripple periodicity on heating and on cooling, the possibility that the radiation effect involves the shift of ripple periodicity is excluded.

In DPPC multilamellar systems Tenchov et al. [13] have reported the formation of the $P_{\beta'}$ (mst) state whose diffraction profile consisted of multiple peaks with low intensity. This phase was observed after cooling through the main transition at a slow scan rate of 0.5 C°/min. In the DMPC system, however, $P_{\beta'}$ (mst) state was not obtained at least on condition that the samples were cooled from about 28°C at a scan rate of 0.03–0.5 C°/min (data not shown). We think that this discrepancy arises from the difference in the hydrocarbon chain length. The condition of the appearance of $P_{\beta'}$ (mst) state will be described in detail elsewhere.

Arrangement of the PC molecules in the membrane has not been established yet. The appearance of the ripple structure should be related to the interaction

between the molecules. Generally the undulated structure with incommensurate wave vector can be explained by taking into account not only the nearest-neighbor interaction but also the second nearest-neighbor interaction. In the case of the ripple structure, the origin of the microscopic molecular interactions should be studied further.

It is of interest to study the temperature dependence of the ripple repeat distance within the framework of the Landau-de Gennes phenomenological theory. Marder et al. [12] have proposed a model explaining the ripple formation, in which they have defined an order parameter t as follows:

$$t = \frac{(d - d_f)}{(d_s - d_f)} \tag{1}$$

where d is the thickness of the membrane at temperature T and d_f and d_s are the thickness of fluid-like and solid-like parts in the membrane, respectively (see Ref. 12). It is assumed that the structure in the liquid-crystalline phase, the ripple phase and the gel phase is characterized in terms of t. In the liquid-crystalline phase $t = 0$ and in the gel phase $t = 1$. In the ripple phase t is modulated as a function of position x in a certain direction on the membrane surface. The spatial modulation of the thickness in the ripple phase, $t(x)$, is expected from the alternative appearance of the ordered region and the disordered region of hydrocarbon chains. This aspect has been predicted experimentally from the measurements of nuclear magnetic resonance [13], fluorescence decay [14] and electron spin resonance [15] as mentioned before.

The free energy expansion as a function $t(x)$ is given by

$$G = G_0 + G_1$$

$$G_0 = \tfrac{1}{2}(\bar{T}t^2 - 2t^3 + t^4) \tag{2}$$

$$G_1 = \tfrac{1}{2}(t'')^2 + \alpha t t'' \tag{3}$$

where $\bar{T}$ is a dimensionless temperature, α is a coupling constant and $'$ denotes spatial derivative. Marder et al. might consider all combination of secondary products generated by t, t' and t''. They analyzed the free energy under the following trial function for t.

$$t(x) = A + B\cos(kx) \tag{4}$$

where k is the ripple wave number, B corresponds to the ripple amplitude. From Eqn. 4 the ripple repeat distance $1/k$ derived to be $\sqrt{1/\alpha}$ which exhibits no temperature dependence.

We first try to consider the higher order harmonics in the order parameter under the above free energy as follows

$$t(x) = A + \sum_n B_n \cos(nkx) \tag{5}$$

TABLE II

All combination of cubic products generated by t, t′ and t″, and their spatial average which should be considered in the Landau-de Gennes free energy per unit area

Cubic products	Spatial average of the cubic products
t^3	(already included in G_0)
$(t')^3$	0
$(t'')^3$	0
$t(t')^2$	$k^2AB^2/2$
$t(t'')^2$	$k^4AB^2/2$
$t'(t'')^2$	0
t^2t'	0
t^2t''	$-k^2AB^2$
$t''(t')^2$	0
$tt't''$	0

In this case, the ripple repeat distance $1/k$ is given by

$$\frac{1}{k} = \left\{ \frac{\alpha \cdot (B_1^2 + 4B_2^2 + \cdots + n^2B_n^2)}{B_1^2 + 16B_2^2 + \cdots + n^4B_n^2} \right\}^{-1/2} \tag{6}$$

However, the variation of the ripple repeat distance expected from Eqn. 6 is at most 0.6%, which is far smaller than the variation of the observed one. Therefore within such extension it is not possible to explain the observed large temperature dependence by G_1 of Eqn. 3.

Second, let us take into account of the higher order terms composed of all combination of cubic products generated by t, t' and t'' in the free energy expansion. The total number of these terms is ${}_3H_3 = 10$. The contribution of them to the free energy is summarized in Table II under the condition that $t = A + B\cos(kx)$. Among the terms giving non-zero free energy, the spatial averages of the terms $t(t')^2$ and t^2t'' give the same form and therefore the independent terms $t(t'')^2$ and $t(t')^2$ should be considered as additional terms to G_1 as follows:

$$G_1 = \tfrac{1}{2}(t'')^2 + \alpha t t'' + \beta t(t'')^2 + \gamma t(t')^2 \tag{7}$$

where β and γ are coupling constants. Assumed that $t = A + B\cos(kx)$, the ripple repeat distance is given by

$$\frac{1}{k} = \sqrt{\frac{1 + 2\beta A}{\alpha - \gamma A}} \tag{8}$$

Under the assumption that $\beta = 0.6$ and $\gamma = 0.6$, the total free energy $G_0 + G_1$ were examined at various α values and its temperature dependences were given in Fig. 4. The free energy G_0 corresponds to that of the phase with uniform order parameter. If the total free energy G is smaller than G_0, the ripple phase appears as seen in Fig. 4. Figs. 5a and b indicate the temperature dependence of the parameters A and B at various

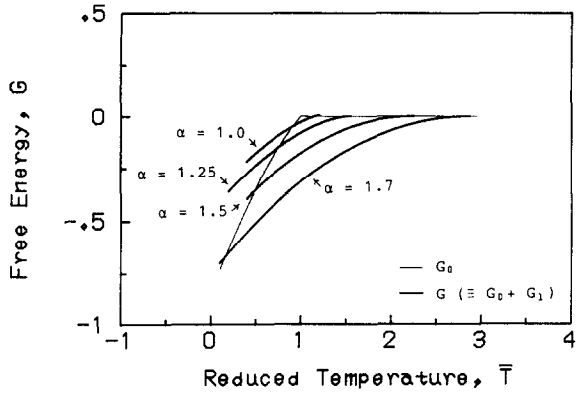

Fig. 4. Calculated free energy per unit area as a function of the reduced temperature $\bar{T}$. The thin line exhibits the free energy for the liquid crystalline phase and for the gel phase given by G_0. The thick lines exhibit the free energy for the ripple phase at various α values, where β and γ are fixed to 0.6.

values of the coupling constants. In Fig. 6 the calculated temperature dependence of the ripple repeat distance is drawn at various values of the coupling constants. As seen in this figure the small value of α generates convex curves as a function of $\bar{T}$. When α increases, it turns to concave nature. The curve at $\alpha = 1.7$ resembles the observed temperature dependence given in Fig. 3. At

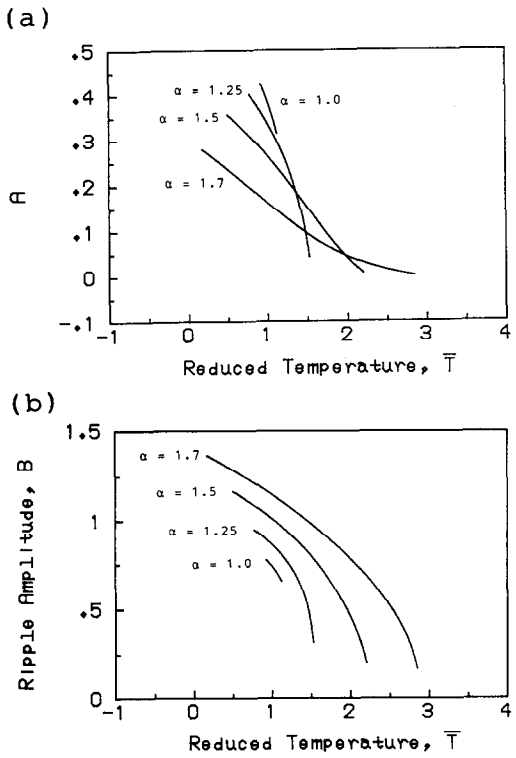

Fig. 5. Calculated values of A and B as a function of the reduced temperature $\bar{T}$ at various α values which are drawn in Figs. 5a and b, respectively. In this calculation, both β and γ are fixed to 0.6.

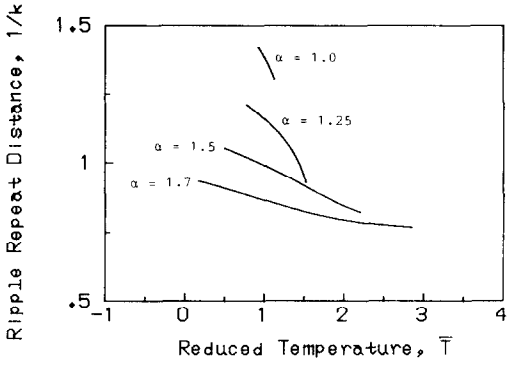

Fig. 6. Calculated ripple repeat distance $(1/k)$ in an arbitrary scale as a function of the reduced temperature $\bar{T}$ at various α values. In this calculation, both β and γ are fixed to 0.6.

$\alpha = 1.7$ the ripple phase lies between $\bar{T} = 0.175$ and $\bar{T} = 2.875$ in the theory. To compare the curve with that of the experiment, we adjust this temperature range to the real temperature range of $P_{\beta'}$ phase from 11°C to 23.5°C and also the ripple repeat distance at $\bar{T} = 2.875$ is 12.1 nm. As seen in Fig. 7 it was found that the solid line theoretically analyzed well explains the experimental results.

In the PC-cholesterol system the ripple repeat distance at a certain temperature increases with cholesterol concentration as pointed out [7]. It is worth while to notice that in the PC-cholesterol system the temperature dependence of the ripple repeat distance was found to be nearly parallel to that of the pure PC from our preliminary experiment of X-ray small-angle diffraction [21]. This fact indicates that the mechanism of the temperature dependence is common between the pure PC and the PC-cholesterol systems. In the PC-cholesterol system, the temperature dependence deviates however from the above tendency near the main transition and in the lower temperature region. The details of the results in the PC-cholesterol system will be published elsewhere.

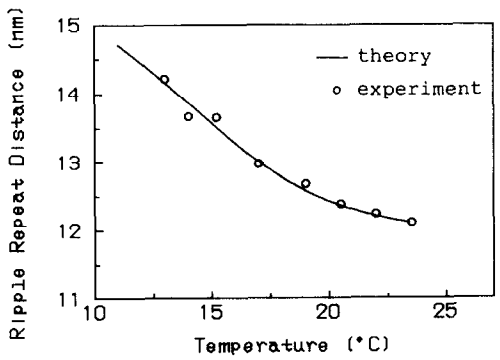

Fig. 7. Solid line represents the calculated ripple repeat distance in the scale adjusted to the experimental value (where $\alpha = 1.7$, $\beta = \gamma = 0.6$) as a function of temperature. Experimental results obtained from small-angle X-ray diffraction are presented by open circles.

Acknowledgments

We are grateful to Dr. Ohki for useful discussions. This work was supported by Grant-in-Aid for Co-operative Research (No. 63300007) from the Japanese Ministry of Education, Science and Culture. We wish to thank the Computation Center of Nagoya University for data analysis.

References

1 Tardieu, A., Luzzati, V. and Reman, F.C. (1973) J. Mol. Biol. 75, 711–733.
2 Janiak, M.J., Small, D.M. and Shipley, G.G. (1976) Biochemistry 15, 4575–4580.
3 Hicks, A., Dinda, M. and Singer, M.A. (1987) Biochim. Biophys. Acta 903, 177–185.
4 Luna, E.J. and McConnell, H.M. (1977) Biochim. Biophys. Acta 466, 381–392.
5 Janiak, M.J., Small, D.M. and Shipley, G.G. (1979) J. Biol. Chem. 254, 6068–6078.
6 Sackmann, E., Ruppel, D. and Gebhardt, C. (1980) Springer Series in Chemical Physics, Vol. 2 (Helfrich, W. and Heppke, G., eds.), pp. 309–326, Springer Verlag, Berlin.
7 Copeland, B.R. and McConnell, H.M. (1980) Biochim. Biophys. Acta 599, 95–109.
8 Zasadzinski, J.A.N., Schneir, J., Gurley, J., Elings, V. and Hansma, P.K. (1988) Nucl. Instrum. Methods 239, 1013–1015.
9 Inoko, Y., Mitsui, T., Ohki, K., Sekiya, T. and Nozawa, Y. (1980) Phys. Stat. Sol. (a) 61, 115–121.
10 Wack, D.C. and Webb, W.W. (1989) Phys. Rev. A 40, 2712–2730.
11 Mortensen, K., Pfeiffer, W., Sackmann, E. and Knoll, W. (1988) Biochim. Biophys. Acta 945, 221–245.
12 Marder, M., Frisch, H.L., Langer, J.S. and McConnell, H.M. (1984) Proc. Natl. Acad. Sci. USA 81, 6559–6560.
13 Wittebort, R.J., Schmidt, C.F. and Griffin, R.G. (1981) Biochemistry 20, 4223–4228.
14 Schneider, M.B., Chan, W.K. and Webb, W.W. (1983) Biophys. J. 43, 157–173.
15 Tsuchida, K. and Hatta, I. (1988) Biochim. Biophys. Acta 945, 73–80.
16 Amemiya, A., Wakabayashi, K., Hamanaka, T., Wakabayashi, T. Matsushita, T. and Hashizume, H. (1983) Nucl. Instrum. Methods 208, 471–477.
17 Nakagawa, T. and Oyanagi, Y. (1980) 'Program System SALS for Nonlinear Least-Squares Fitting in Experimental Sciences' in Recent Developments in Statistical Inference and Data Analysis (Matusita, K., ed.) pp. 221–225, North Holland, Amsterdam.
18 Lewis, R.N.A.H., Mak, N. and McElhaney, N. (1987) Biochemistry 26, 6118–6126.
19 Caffrey, M. (1984) Nucl. Instrum. Methods. 222, 329–338.
20 Tenchov, B.G., Yao, H. and Hatta, I. (1989) Biophys. J. 56, 757–768.
21 Matuoka, S., Kato, S., Akiyama, M., Amemiya, Y. and Hatta I. (1988) in Photon Factory Activity Report, p. 121, National Laboratory for High Energy Physics, Tsukuba Japan.